JOURNAL OF MATERIALS SCIENCE 29 (1994) 4860–4865

Microstructure of mechanically alloyed Al–In alloys

K. UENISHI, H. KAWAGUCHI, K. F. KOBAYASHI
Department of Welding and Production Engineering, Osaka University, Yamadaoka 2-1, Suita, Osaka 565, Japan

Mechanical alloying (MA) starting from elemental powder mixtures was performed on immiscible Al–10, 30 and 50 at % In alloys. Al and In were finely mixed with increasing MA time and the crystal size of each element became up to 40 nm after MA for 1152 ks. With refinement of the structure, the hardness increased up to 120 H_V in Al–10 at % In alloy, a value larger than that obtained from the rule of mixtures. The melting temperature of In was recognized, by thermal analyses, to fall by about 3 K for mechanically alloyed Al–In alloy, showing the possibility of forming f.c.t In supersaturated solid solution. A new endothermal peak around 420 K, which corresponded with the melting temperature of metastable f.c.c. In, was recognized for mechanically alloyed Al–50 at % In alloy.

1. Introduction

Mechanical alloying (MA) was first introduced by Benjamin [1] to produce metal composite powders from mixtures of elemental powders. By repetitive fracturing and cold welding of constituent powders, finely and homogeneously alloyed material can be obtained even in the immiscible alloy systems in which alloying is impossible by the normal casting technique [2]. Moreover, MA has attracted attention as a new method to obtain non-equilibrium alloys [3, 4] since Koch [5] first showed amorphization in the Ni–Nb system by MA. This amorphization was considered to be metastable melting from the mixture of elemental powders [6] and the driving force a negative heat of mixing of the alloy system. That is why this amorphization was intensively researched in the alloy systems with negative heat of mixing. However, since Schwarz first reported the amorphization by mechanical grinding of equilibrium intermetallic compounds [7], MA was recognized to include an energizing process and it began to be considered that it is possible to form non-equilibrium alloys even in systems with a positive heat of mixing [8]. The authors have reported the formation of a non-equilibrium phase in immiscible Ag–Cu [9], Fe–Cu [10] and Fe–Ag–Cu [11] systems.

In this work, MA was performed in the immiscible Al–In alloy system [12] with a positive heat of mixing, 24 kJ mol^{-1} [13]. Changes of structure and hardness were examined as a function of MA time or alloying composition. X-ray diffraction or differential scanning calorimetry analysis was performed to identify the phases formed by MA.

2. Experimental procedure

Elemental powders of Al (purity 99% and particle size 100 μm) and In (purity 99.9% and particle size 30 μm) were used as starting materials. These powders were mixed to the desired compositions. Mechanical alloying was performed in a vibrating ball mill (Nisshin Gikken, MISUNI NEV-MA8) at a vibration rate of 13.1 Hz. The vial and balls used for milling were made of SUS304 stainless steel. The size of vial was 55 mm inner diameter and 40 mm height and the capacity was 900 cm^3. The balls were 11 mm in diameter. Mixed powders were sealed in the vial with balls in an argon atmosphere. The balls to powder weight ratio was about 30:1. To avoid the adhesion of powder to the balls and vial, about 1 cm^3 of ethyl alcohol was added to the sample powder. Cooling the vial by flowing water prevented temperature rise of the vial due to ball–ball or ball–vial collisions.

To follow the changes in powders during MA, powders were mechanically alloyed for various lengths of time without any intervals. The structure of the powder obtained was observed by scanning electron microscopy (SEM) and by transmission electron microscopy (TEM). The composition was chemically analysed by the inductively coupled plasma method (ICP). Changes in hardness were investigated with MA time by measurements of the Vickers hardness. Powder X-ray diffraction (XRD) analysis using CoK_α radiation was performed to identify the phases formed by MA. MA powders were thermally analysed by differential scanning calorimetry (DSC; Perkin Elmer DSC-7) at a heating rate of 0.33 $K s^{-1}$.

3. Results and discussion

Fig. 1 shows the microstructural evolution of Al–50 at % In powders by MA. The morphology of starting Al and In powders was nearly spherical. At the initial stage of MA, for example 3.6 ks MA, both elements (Al is contrasted in black, In in white) were flattened by

0022–2461

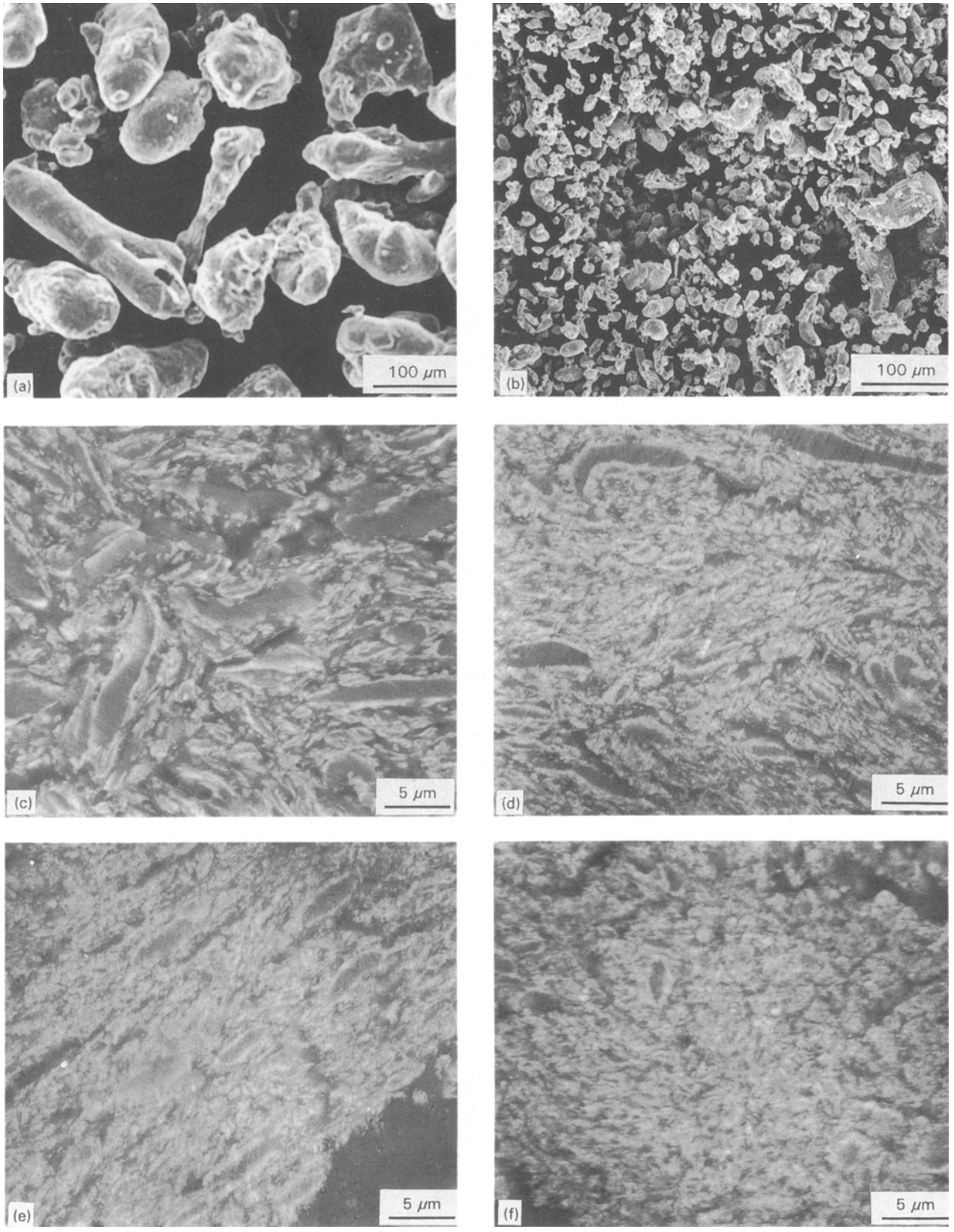

Figure 1 Microstructural evolution of Al–50 at % In powders by MA: (a) starting Al, (b) starting In, (c) MA 3.6 ks, (d) MA 10.8 ks, (e) MA 18 ks, (f) MA 36 ks.

repetitive rolling and were mixed by cold welding. As Al and In are ductile, rolling or cold welding dominantly occurs in comparison with fracturing at the early stage of MA. By further milling, powders were hardened by intensive cold working and flattened elements were fractured to a spherical shape. The grain size of In decreased faster than that of Al because Al is harder than In. After MA for 36 ks, each element was mixed to sub-micrometre order. Fig. 2 shows the changes of lamellar spacing of Al–In powders for various compositions as a function of MA time. The spacing rapidly decreased at the early stage of MA and

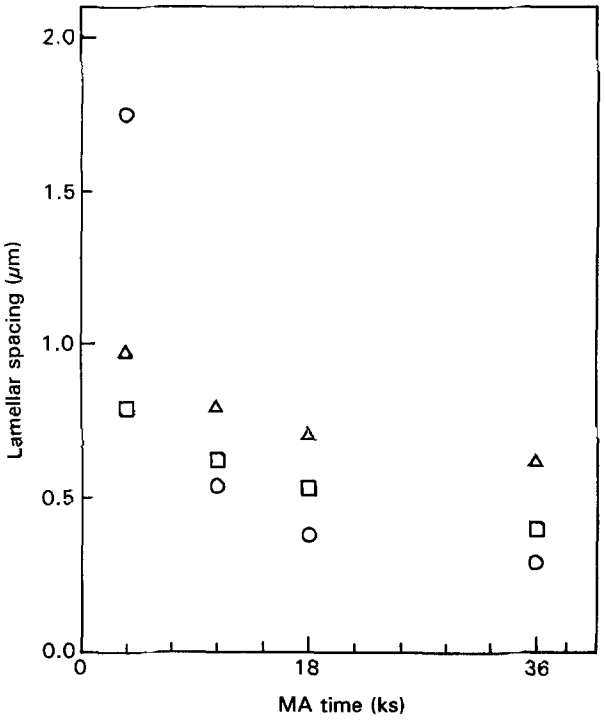

Figure 2 Changes of lamellar spacing observed in mechanically alloyed Al–In powders as a function of MA time: (○) Al–10 at % In, (△) Al–30 at % In, (□) Al–50 at % In.

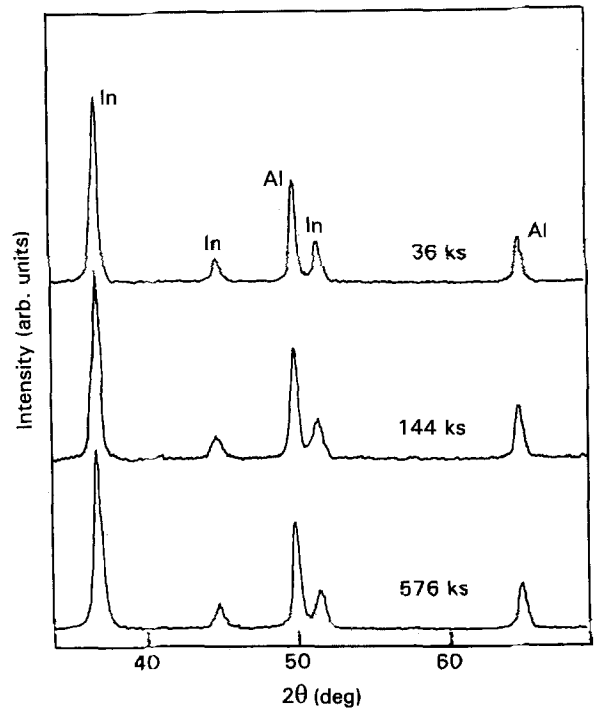

Figure 3 Changes of XRD pattern of Al–10 at % In powders as a function of MA time.

with increasing MA time the rate of reduction became smaller. By MA for 36 ks, the lamellar spacing reached a minimum value of about 0.4 μm with no relation to the composition, and this value remained almost constant on further MA up to 288 ks.

Fig. 3 shows the changes of XRD pattern of Al–10 at % In alloy as a function of MA time. Only peaks from pure Al and In were detected and no shift of peak position was recognized. With increasing MA time these diffraction peaks became broader, showing refinement of the crystallites. Fig. 4 shows the changes of Al or In crystallite size calculated from the Scherrer formula [14] as a function of milling time. As well as the changes of lamellar spacing shown in Fig. 2, the crystallite size rapidly decreased at an early stage of MA and it gradually reached a minimum constant value. The minimum value of Al crystallite size was 40 nm, which value was almost the same as that of In,

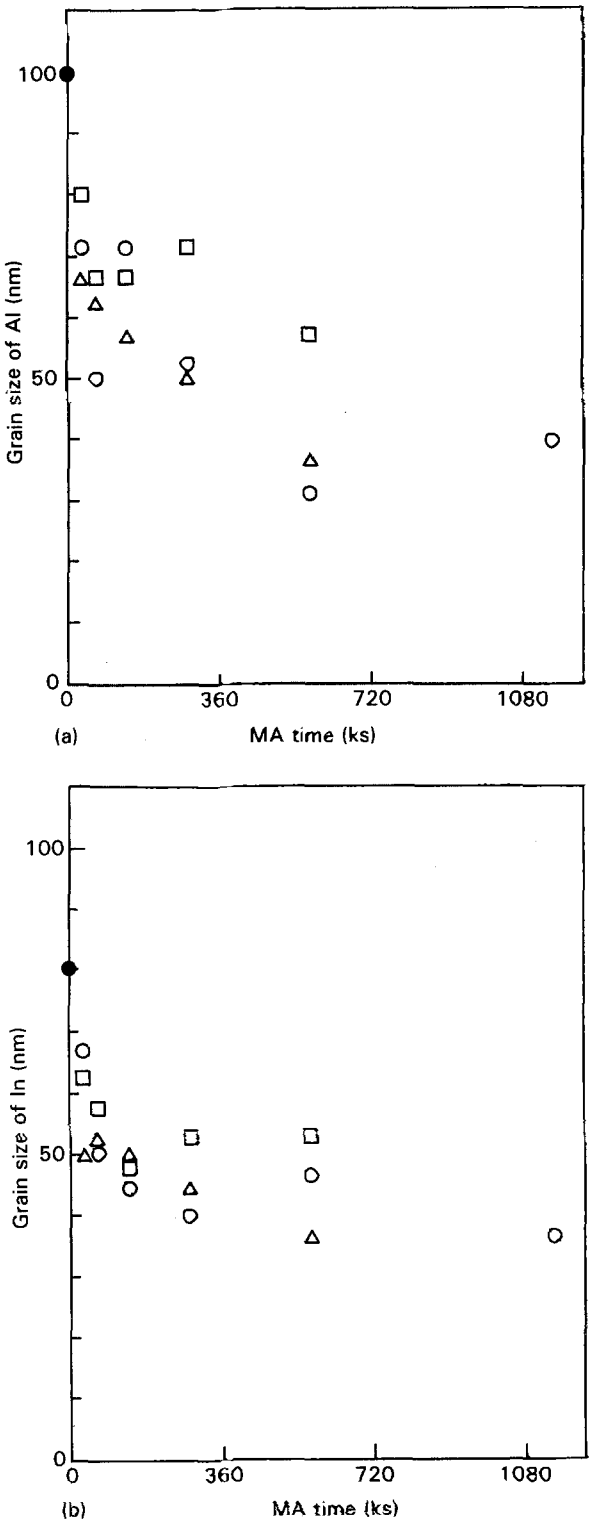

Figure 4 Changes of the grain size of (a) Al and (b) In as a function of MA time: (●) Al or In, (○) Al–10 at % In, (△) Al–30 at % In, (□) Al–50 at % In.

but refinement of the In crystallites was faster than for Al. With increasing In composition, refinement of the crystallites became slower. Fig. 5 shows the TEM image of Al–50 at % In powder mechanically alloyed for 36 ks. Equiaxed In was dispersed in an Al matrix and the grain size of In was about 40 nm, which corresponds well with the value evaluated from the half-value width of the XRD peak.

Fig. 6 shows the changes of Vickers hardness of Al–In MA powder for various compositions as a function of MA time. Cold working and refinement of each elements resulted in an increase of hardness. The hardness rapidly increased at the early stage of MA but with further MA it gradually reached a maximum constant value. The maximum value increased on increasing the harder Al content and it was much larger than that expected from the rule of mixtures in all of the compositions.

Fig. 7 shows DSC curves of Al–50 at % In powders mechanically alloyed for 36 ks. MA powders were heated up to 973 K at a heating rate of 0.33 Ks^{-1} (first run) and they were heated again under the same conditions (second run) after cooling from 973 to 323 K. The mechanically alloyed powder completely melted at 973 K, so the DSC curve for the second run can be considered to show the thermogram of Al–50 at % In alloy in an equilibrium state. In fact, there were no peaks except endothermal peaks due to melting of In at 429 K and melting of Al at 911 K. In the first run, the In melting temperature can be seen to be depressed in comparison with the second run. This depression of the melting temperature of In can be observed in Al–10 at % In and Al–30 at % In MA powders, too.

Fig. 8 shows the changes of melting temperature depression as a function of MA time and alloy composition. The depression increased with MA time and

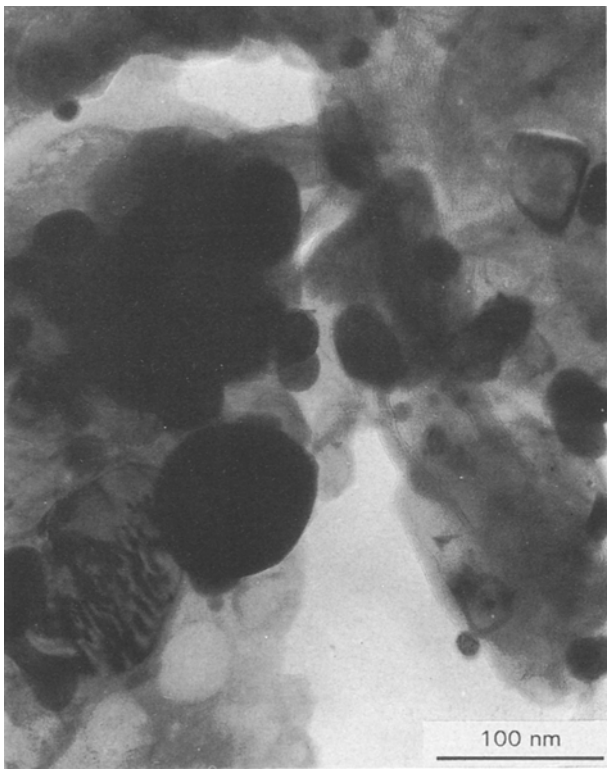

Figure 5 TEM image of an Al–10 at % In powder mechanically alloyed for 2048 ks.

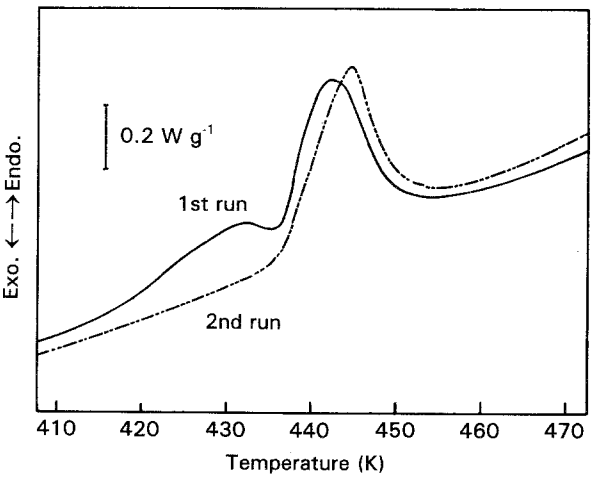

Figure 7 DSC curves of Al–50 at % In powders mechanically alloyed for 36 ks. The sample was heated up to 973 K at a rate of 0.33 $K s^{-1}$ (1st run), cooled down to 123 K and then heated again under the same conditions (2nd run).

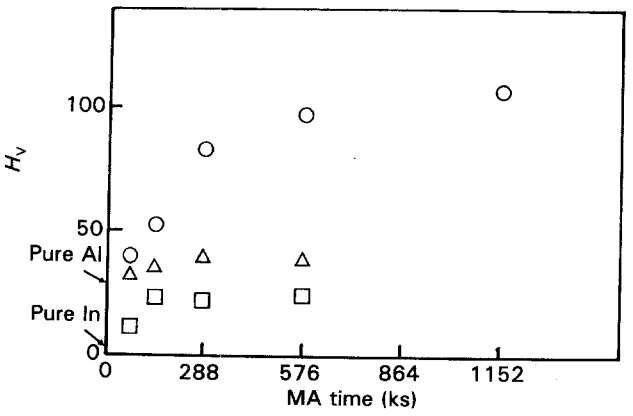

Figure 6 Changes of Vickers hardness H_v (load 0.245 N) of Al–In powders as a function of MA time: (○) Al–10 at % In, (△) Al–30 at % In, (□) Al–50 at % In.

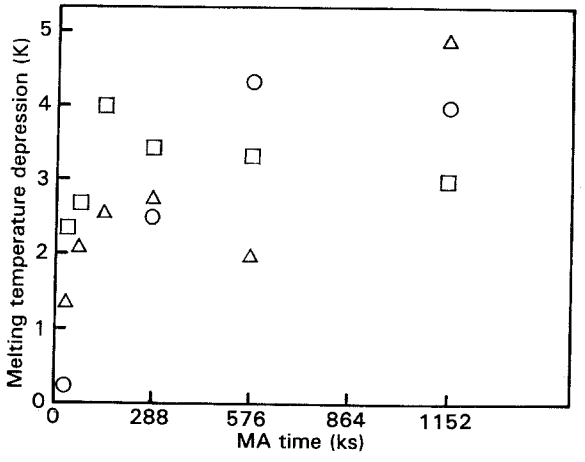

Figure 8 Changes in the melting temperature depression of In for mechanically alloyed Al–In alloy as a function of MA time: (○) Al–10 at % In, (△) Al–30 at % In, (□) Al–50 at % In.

gradually reached a maximum constant value. The relation between maximum depression and alloy composition cannot be obtained due to the uncertainty of the baseline, but a depression about 3 K was recognized in the entire composition range examined in this work. Koch *et al.* [15] reported the depression of Sn melting point in mechanically alloyed Sn–Ge powders. Like the Al–In system, Sn–Ge is an immiscible alloy system and the reason for the depression is believed to be the interfacial area increases attained by MA. Certainly, the melting temperature of nanometre-sized crystals is known to be lower than for bulk crystal in pure metals and in many alloy systems. According to Allen *et al.* [16], the melting temperature T_{mf} of pure nanometre-sized crystals can be described as follows:

$$\frac{T_{mf}}{T_0} = 1 - \frac{K}{r}$$

where T_0 is the melting temperature of bulk crystal and r the grain size. K is a constant value determined by the element and in the case of In it is about 0.23 nm. By using the grain size of In as 40 nm, which was confirmed by XRD analysis and TEM observation, the depression can be calculated to be 3 K, which corresponds fairly well with the experimental data.

In the Al–In system, however, the melting temperature of In is reported to rise with decreasing In grain size because the wetting angle between liquid In and solid Al is smaller than 90° [17], so it was concluded that fine dispersion of In in Al is not a reason for this melting temperature depression. The effect of contamination introduced during MA must be considered as one of the reasons. Table I shows the results of chemical analysis for Al–10 at % In powder mechanically alloyed for 1152 ks. Fe, Cr and Ni are contaminants from the stainless steel balls and vial. Oxygen may be considered to come from ethyl alcohol or from surface oxidation during analysis. However, in our investigation the solubility of Fe, Cr and O in In is negligibly small and Ni never lowers the melting temperature of In because In solidifies by a peritectic reaction. Such a depression was previously observed in our research on Al–In alloy rapidly quenched by the gun method. It may be considered that the effect of contamination is small and that the supersaturated solid solution of Al in In is the reason for the depression, because the depression can be observed even in a rapidly quenched alloy with small contamination.

Fig. 9 shows an estimated metastable phase diagram for the In-rich side of the Al–In alloy system. By MA or rapid quenching a non-equilibrium In solid solution was formed, which depressed the melting temperature of In. The non-equilibrium solid solubility can be estimated by extrapolation of the solidus line shown in Fig. 9, but it cannot be measured because the equilibrium solid solubility is only reported to be negligibly small without a concrete value being given. Judging from the large gradient of the solidus line, the solubility may also be small, which could give no shift in the XRD peak positions.

TABLE I Chemically analysed composition (at %) of Al–10 at % In powder mechanically alloyed for 1152 ks.

Fe	Cr	Ni	Al	In	O
0.31	0.07	0.04	84	9.4	6.6

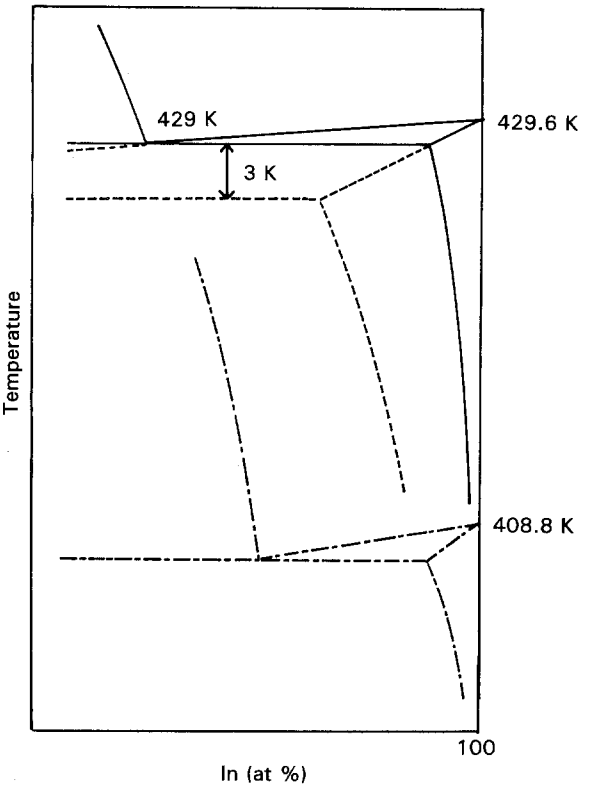

Figure 9 Schematic phase diagram for (——) equilibrium Al–f.c.t. In, (– – –) metastable Al–supersaturated f.c.t. In (– · –) and metastable Al–f.c.c. In.

As shown in Fig. 7, a broad and small new endothermal peak can be detected from about 410 to 435 K. This endothermal peak was observed only in Al–50 at % In MA powders. According to thermodynamical data reported by Kaufman *et al.* [18], the free energy of f.c.c. and liquid In can be obtained from the equation.

$$G_{In}^{L-f.c.c.} = -2908 + 7.113T \quad (J\,mol^{-1})$$

By using this equation the melting temperature of metastable f.c.c. In can be calculated to be 409 K, which corresponds well with the melting temperature observed in DSC curves. Metastable f.c.c. In is found to precipitate from Al-rich Al–In alloy by ageing it below 300 K [19]. Although f.c.c. In is a metastable phase, the free energy gap between f.c.c. and the equilibrium f.c.t. phase is only about 0.4 kJ mol^{-1} at room temperature [19]. MA is reported, for example in the amorphization of intermetallic compounds by mechanical grinding, to be able to energize the alloy system, so an f.c.t. to f.c.c. transition may occur.

As mentioned above, results suggesting the formation of a non-equilibrium solid solution or of metastable f.c.c. In were obtained by DSC studies, but the solubility was not large and the free energy rise was only about a few hundred J mol^{-1}. The authors have reported that the Fe–Cu alloy system was energized up to about 10 kJ mol^{-1} by MA [10]. Alloys

were considered to be energized by refinement of each element with an increase of interfacial energy. Although Fe and Cu were refined to nanometre dimensions, the crystallite size of Al–In alloys was 40 nm because Al and In are ductile and easily recrystallize even around room temperature. This difference of refinement is considered to give the difference in energized free energy.

4. Conclusions

Immiscible Al–In alloys were mechanically alloyed by vibrating ball milling. The alloying behaviour was monitored by structure observation, measurements of hardness, XRD analyses and DSC studies. The results are as follows:

1. Al and In were finely mixed with increasing MA time and the grain size reached 40 nm by MA for 288 ks.
2. The hardness increased with MA time due to repeated cold work and refinement of each element. The hardness was much larger than that estimated from the rule of mixtures.
3. The melting temperature was recognized to depress by about 3 K, suggesting a supersaturated solid solution of Al in In.
4. A new endothermal peak starting from about 405 K was recognized in mechanically alloyed Al–50 at % In powders. The temperature corresponded well with the melting temperature of metastable f.c.c. In.

Acknowledgements

The authors thank Dr T. Tanaka, Osaka Sangyo University, for experimental assistance in the sample preparation for TEM observation, Messrs Y. Hayashi and S. Kashiwai, Hyogo Prefectural Research Institute, for TEM observation and Mr J. Saida, Nisshin Steel, for chemical analysis.

References

1. J. S. BENJAMIN, *Metall. Trans.* **1** (1970) 2943.
2. P. S. JILMAN and J. S. BENJAMIN, *Ann. Rev. Mater. Sci.* **13** (1983) 1791.
3. K. F. KOBAYASHI, N. TACHIBANA and P. H. SHINGU, *J. Mater. Sci.* **25** (1990) 3149.
4. M. V. ZDUJIC, K. F. KOBAYASHI and P. H. SHINGU, *ibid.* **26** (1991) 5502.
5. C. C. KOCH, O. B. CAVIN, C. G. MCKAMEY and J. O. SCARBROUGH, *Appl. Phys. Lett.* **43** (1983) 1017.
6. R. B. SCHWARZ, R. R. PETRICH and C. K. SAW, *J. Non-Cryst. Solids* **76** (1985) 281.
7. R. B. SCHWARZ and C. C. KOCH, *Appl. Phys. Lett.* **49** (1986) 146.
8. E. GAFFET, *Mater. Sci. Eng.* **A134** (1991) 1380.
9. K. UENISHI, K. F. KOBAYASHI, K. N. ISHIHARA and P. H. SHINGU, *ibid.* **A134** (1991) 1342.
10. K. UENISHI, K. F. KOBAYASHI, S. NASU, H. HATANO, K. N. ISHIHARA and P. H. SHINGU, *Z. Metallkde* **83** (2) (1992) 132.
11. K. UENISHI, K. F. KOBAYASHI, K. N. ISHIHARA and P. H. SHINGU, *Mater. Sci. Forum* **88–90** (1992) 459.
12. J. L. MURRAY, in "Binary Alloy Phase Diagrams," Vol. 1 (American Society for Metals, Ohio, 1983) p. 121.
13. A. K. NIESSEN, F. R. DE BOER, R. BOOM, P. F. DE CHATEL, W. C. M. MATTENS and A. R. MIEDEMA, *CALPHAD* **7** (1) (1983) 51.
14. B. D. CULITY, in "Elements of X-ray diffraction" (Addision-Wesley, Massachusetts, USA, 1987) p. 102.
15. C. C. KOCH, J. S. C. JANG and S. S. GROSS, *J. Mater. Res.* **4** (1989) 557.
16. G. L. ALLEN, R. A. BAYLES, W. W. GILE and W. A. JESSER, *Thin Solid Films* **144** (1986) 297.
17. H. SAKA, *J. Jpn Inst. Met.* **31** (9) (1992) 204.
18. L. KAUFMAN, J. NELL, K. TAYLOR and F. HAYES, *CALPHAD* **5** (3) (1981) 185.
19. J. M. SILCOCK, *J. Inst. Met.* **84** (1955) 19.

Received 26 January 1993
and accepted 21 March 1994